Journal of Molecular Cell Biology (2023), 15(4), mjad025 https://doi.org/10.1093/jmcb/mjad025
Published online April 18, 2023

Article

CSF2 upregulates CXCL3 expression in adipocytes to promote metastasis of breast cancer via the FAK signaling pathway

Xi He[1,†], Lieliang Wang[2,†], Honghui Li[1], Yaru Liu[1], Chang Tong[3], Caifeng Xie[1], Xiaohua Yan[1], Daya Luo[1], and Xiangyang Xiong[1,4,*]

[1] Department of Biochemistry and Molecular Biology, School of Basic Medical Sciences, Nanchang University, Nanchang 330006, China
[2] Department of Breast Surgery, Jiangxi Cancer Hospital, Nanchang 330029, China
[3] Pediatric Medical School, Nanchang University, Nanchang 330031, China
[4] Province Key Laboratory of Tumor Pathogens and Molecular Pathology, Nanchang University, Nanchang 330006, China
[†] These authors contributed equally to this work.
* Correspondence to: Xiangyang Xiong, E-mail: xiangyangxiong@ncu.edu.cn

Edited by Hua Lu

Recent studies have demonstrated that cancer-associated adipocytes (CAAs) in the tumor microenvironment are involved in the malignant progression of breast cancer. However, the underlying mechanism of CAA formation and its effects on the development of breast cancer are still unknown. Here, we show that CSF2 is highly expressed in both CAAs and breast cancer cells. CSF2 promotes inflammatory phenotypic changes of adipocytes through the Stat3 signaling pathway, leading to the secretion of multiple cytokines and proteases, particularly C–X–C motif chemokine ligand 3 (CXCL3). Adipocyte-derived CXCL3 binds to its specific receptor CXCR2 on breast cancer cells and activates the FAK pathway, enhancing the mesenchymal phenotype, migration, and invasion of breast cancer cells. In addition, a combination treatment targeting CSF2 and CXCR2 shows a synergistic inhibitory effect on adipocyte-induced lung metastasis of mouse 4T1 cells *in vivo*. These findings elucidate a novel mechanism of breast cancer metastasis and provide a potential therapeutic strategy for breast cancer metastasis.

Keywords: breast cancer metastasis, cancer-associated adipocytes, CSF2, CXCL3, FAK

Introduction

Breast cancer is one of the most common cancers with higher incidence and mortality rates among women (Wilkinson and Gathani, 2022). Among different breast cancer subtypes, triple-negative breast cancer is characterized by high invasiveness, poor survival, and onset at a younger age (Sharma, 2016). Recent studies have demonstrated that the tumor microenvironment plays an important role in the development of breast cancer. Therefore, much research effort has been put into understanding the molecular drivers of the tumor microenvironment, particularly those involved in the invasion and metastasis.

The tumor microenvironment consists of tumor cells, stromal cells, extracellular matrix (ECM), and blood vessels (Wiseman and Werb, 2002). Some stromal cells in the tumor microenvironment, such as fibroblasts, macrophages, and adipocytes, are involved in the progression of cancers (Anderson and Simon, 2020). Adipocytes are the most abundant stromal cells in breast cancer microenvironment (Tan et al., 2011). Breast cancer cells can induce the adjacent adipocytes into cancer-associated adipocytes (CAAs; Dirat et al., 2011), which display a fibroblast phenotype, including the reduced amount of intracellular lipid droplets and decreased expression of adipocyte differentiation markers such as peroxisome proliferator-activated receptor gamma (PPAR-γ), CCAAT enhancer binding protein alpha (C/EBP-α), and fatty acid-binding protein 4 (FABP4). More importantly, CAAs can secrete a large number of proteases, such as PAI-1 and matrix metalloproteinases (MMPs), and cytokines including IL-6, CCL2, CCL5, and TNF-α, which promote the migration and invasion of breast cancer cells (Dirat et al., 2011; Wu et al., 2019).

Received October 24, 2022. Revised April 12, 2023. Accepted April 17, 2023.

Our previous studies also disclosed the potential role of CAAs in breast cancer progression by activating Stat3 (Liu et al., 2020). Considering the bidirectional interaction between breast cancer cells and CAAs, it is necessary to further explore how breast cancer cells promote the conversion of adipocytes into CAAs.

Granulocyte-macrophage colony-stimulating factor (GM-CSF, also known as CSF2) is a member of the CSF family, which can be produced and secreted by different cell types, including cancer cells (Fleetwood et al., 2005; Hong, 2016). CSF2 binds to its specific receptors CSF2Rα and CSF2Rβ and activates downstream signaling pathways, such as JAK2/Stat3, ERK, NF-κB, and AKT, to elicit biological functions (Hamilton, 2020). In gastric cancer, CSF2 mediates chemotherapy-induced cancer cell stemness via the miRNA–JAK2/Stat3 signaling pathway, leading to tumor progression (Xiang et al., 2022). In pancreatic cancer, CSF2 promotes pancreatic cancer-associated macrophage polarization and helps maintain metabolic homeostasis via the PI3K/AKT pathway (Boyer et al., 2022). However, the role of CSF2 in the microenvironment of breast cancer remains unclear.

In this study, we determined the increased CSF2 expression in adipocytes and breast cancer cells in the tumor microenvironment and how CSF2 regulates C–X–C motif chemokine ligand 3 (CXCL3) in adipocytes and the focal adhesion kinase (FAK) pathway in breast cancer cells to promote breast cancer lung metastasis *in vivo*.

Results

CSF2 is highly expressed in adipocytes and tumor cells after co-culture

Compared to adipocytes cultured alone, adipocytes co-cultured with MDA-MB-231 breast cancer cells showed significantly decreased levels of adipocyte differentiation markers, including PPAR-γ, C/EBP-α, and FABP4 and significantly increased levels of inflammatory factors, such as IL-6, IL-1β, and CCL2 (Supplementary Figure S1 A and B). Oil Red O staining demonstrated smaller volume and number of lipid droplets in the co-cultured adipocytes (Supplementary Figure S1C). These results indicate that breast cancer cells may promote the phenotypic change from adipocytes to CAAs.

Our recent RNA-seq data demonstrated an increased expression level of CSF2 in CAAs compared to that in control adipocytes (Liu et al., 2020), but whether it promotes breast cancer metastasis remains unknown. Previous studies showed that both preadipocytes and mature adipocytes in the tumor microenvironment can interact with tumor cells to promote tumor metastasis (Moreira et al., 2015; Kim et al., 2018; Al-Khalaf et al., 2019). Here, we observed that both CSF2 expression (Figure 1A and C) and secretion (Figure 1B and D) were increased in preadipocytes or adipocytes co-cultured with MDA-MB-231 cells. Further analysis revealed that CSF2 expression was more upregulated in mature adipocytes (12.1-fold) than in preadipocytes (2.6-fold). Therefore, in this study, we focused on the biological role of CSF2 in mature adipocytes.

Next, mature adipocytes were co-cultured with human breast cancer cell line MDA-MB-231, BT549, T47D, or MCF-7 or human normal mammary epithelial cell line MCF10A. Quantitative polymerase chain reaction (q-PCR) and enzyme-linked immunosorbent assay (ELISA) showed that CSF2 expression and secretion were significantly upregulated in adipocytes co-cultured with breast cancer cells but not significantly changed in adipocytes co-cultured with MCF10A cells (Figure 1E and F). These findings, together with breast cancer cell-induced phenotypic change from adipocytes to CAAs, suggest that CSF2 is highly expressed in CAAs.

Previous studies showed that tumor cells can secrete CSF2 (Su et al., 2021). In this study, we found that CSF2 expression and secretion were significantly increased in MDA-MB-231 and BT549 cells co-cultured with adipocytes (Figure 1G and H). We also found that CSF2 mRNA expression level was significantly higher in breast cancer tissues that in normal mammary tissues (Figure 1I; Supplementary Table S1). These results indicate that the expression and secretion of CSF2 are significantly increased in breast cancer cells and adipocytes after co-culture.

CSF2 upregulates CXCL3 expression in CAAs by activating Stat3 signaling

Previous studies demonstrated that CSF2 promotes the inflammation of adipose tissue, while CSF2 knockout reduces the expression of pro-inflammatory cytokines IL-1β, TNF-α, and macrophage inflammatory protein-1α (MIP1α) in the mesenteric adipose of mice (Kim et al., 2008), suggesting that CSF2 may play a role in the activation of CAAs. As shown in Figure 2A, the expression levels of CSF2-specific receptors CSF2Rα and CSF2Rβ were upregulated in adipocytes co-cultured with MDA-MB-231 cells, suggesting that adipocytes respond to endogenous CSF2 stimulation. In addition, recombinant human CSF2 (rhCSF2) treatment increased the expression of several cytokines (IL-6, IL-1β, CCL2, etc.) and chemokines (CXCL1, CXCL2, CXCL3, and CXCL8), of which CXCL3 was the most significantly upregulated (Figure 2B), and also enhanced the secretion of CXCLs in adipocytes (Figure 2C). Meanwhile, rhCSF2 treatment did not markedly affect PPAR-γ and C/EBP-α expression (Supplementary Figure S2A) or lipid droplet size (Supplementary Figure S2B) but significantly upregulated the expression of the proteases PAI-1 and MMPs in adipocytes (Supplementary Figure S2C). These results suggest that CSF2 affects the expression of inflammatory factors and proteases in adipocytes but not adipocyte differentiation. We also found that the mRNA levels of IL-6, CSF2, CXCL1, CXCL2, CXCL3, and CXCL8 in the paracancerous adipose tissues from human breast cancer specimens were significantly higher than that in normal adipose tissues (Figure 2D). Previous studies showed that adipokines adiponectin (APN; Dirat et al., 2011) and Omentin-1 (Zhou et al., 2020) are anti-inflammatory. Here, neither APN nor Omentin-1 was differentially expressed in paracancerous adipose tissues from breast cancer specimens (Supplementary Figure S2D and E).

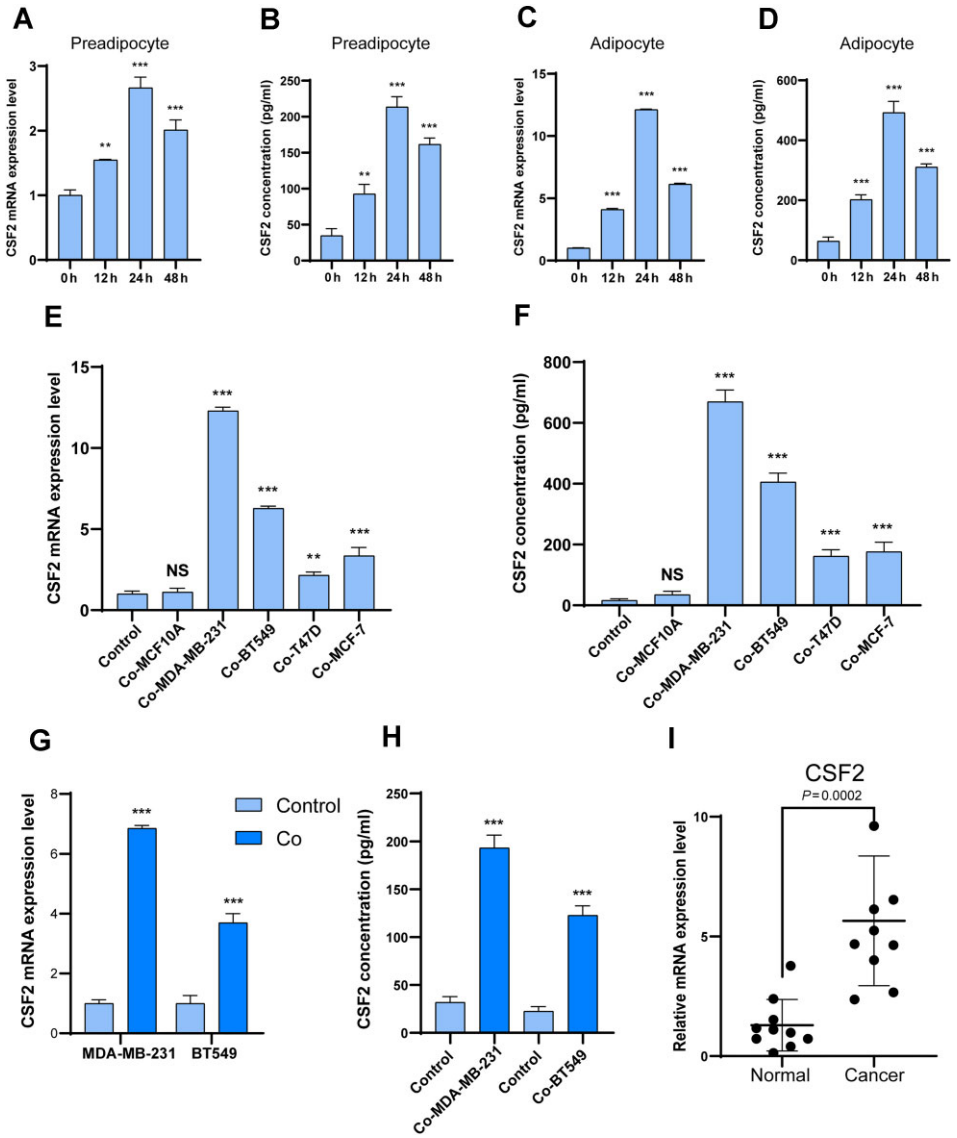

Figure 1 CSF2 is highly expressed in adipocytes and tumor cells after co-culture. (**A** and **B**) The expression (**A**) and secretion (**B**) of CSF2 in preadipocytes co-cultured with MDA-MB-231 cells for 0, 12, 24, and 48 h were measured by q-PCR and ELISA, respectively. (**C** and **D**) The expression (**C**) and secretion (**D**) of CSF2 in adipocytes co-cultured with MDA-MB-231 cells for 0, 12, 24, and 48 h. (**E** and **F**) Adipocytes were co-cultured with different breast cancer cells or normal mammary epithelial cells (MCF10A), and the expression (**E**) and secretion (**F**) of CSF2 were measured. (**G** and **H**) The expression (**G**) and secretion (**H**) of CSF2 in MDA-MB-231 and BT549 cells co-cultured with adipocytes. The relevant MDA-MB-231 or BT549 cells cultured alone served as the control. (**I**) The mRNA expression levels of CSF2 in normal mammary and breast cancer tissues were measured by q-PCR. $***P < 0.001$, $**P < 0.01$, $*P < 0.05$, and NS ($P > 0.05$); $n = 3$.

These results suggest that the increased CSF2 expression and secretion in both CAAs and tumor cells may promote the secretion of cytokines, particularly CXCL3.

We further investigated the underlying mechanism of CXCL3 induction by CSF2. Stat3 is one of the major downstream signaling pathways of CSF2 (Thorn et al., 2016). Our q-PCR results showed that rhCSF2 upregulated the expression of CXCL3 in adipocytes, whereas stattic, a specific inhibitor of Stat3, inhibited CSF2-induced upregulation of CXCL3 (Figure 2E). Western blotting results showed that rhCSF2 also markedly increased the level of Stat3 tyrosine-705 phosphorylation in adipocytes, whereas stattic inhibited CSF2-induced Stat3 phosphorylation (Figure 2F). To investigate the regulation of CXCL3 expression in CAAs by endogenous CSF2, we co-cultured adipocytes with breast cancer cells and treated them with CSF2-neutralizing antibody. As shown in Figure 2G and H, the enhanced CXCL3 expression and Stat3 phosphorylation in CAAs were both inhibited by CSF2-neutralizing antibody. In addition, CXCL3 expression in CAAs was also significantly reduced by stattic treatment (Supplementary Figure S2F). These results suggest that CSF2 activates the Stat3 signaling pathway to upregulate the expression of cytokines such as CXCL3 in CAAs.

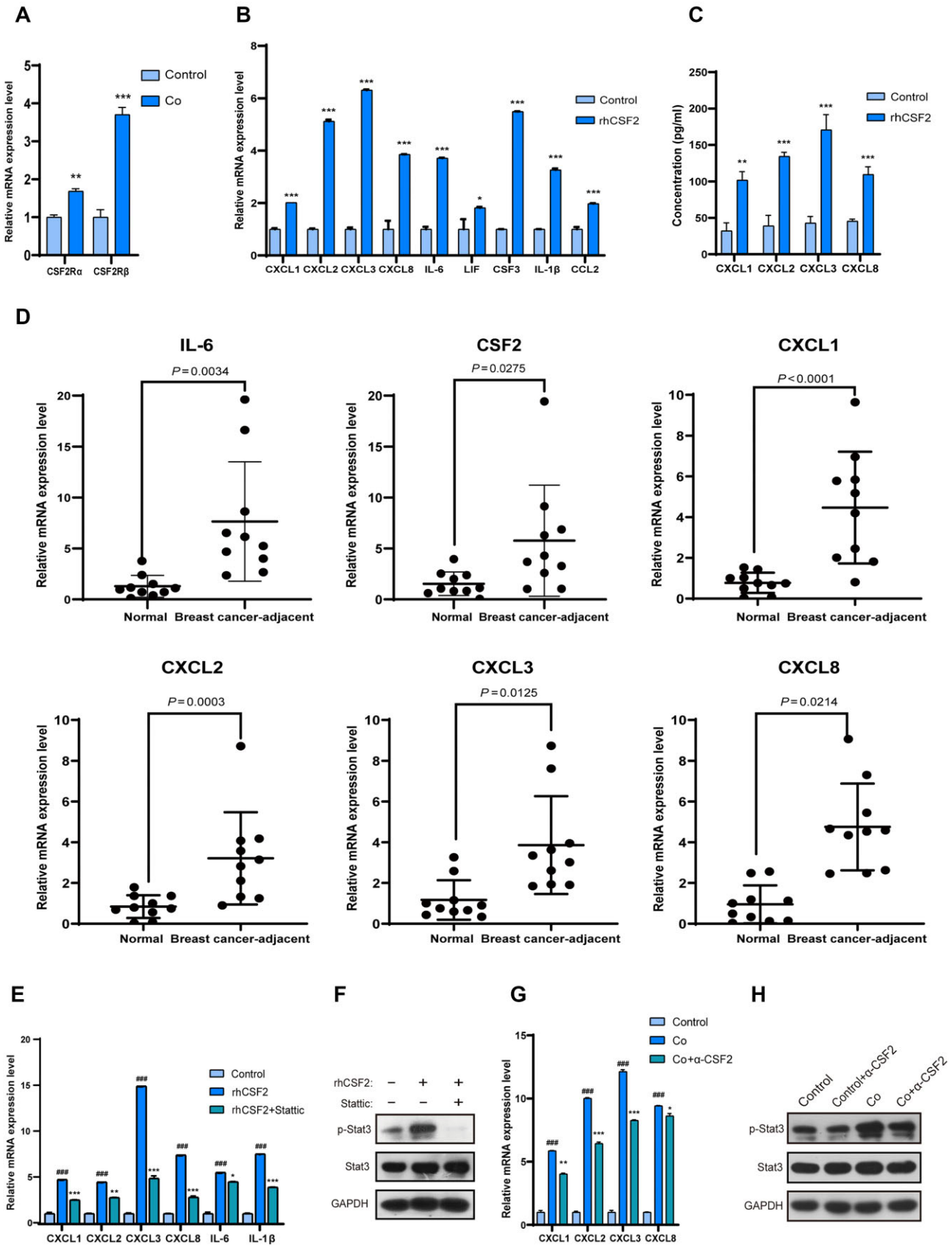
A
Relative mRNA expression level
Control
Co
CSF2Rα
CSF2Rβ
B
Relative mRNA expression level
Control
rhCSF2
CXCL1 CXCL2 CXCL3 CXCL8 IL-6 LIF CSF3 IL-1β CCL2
C
Concentration (pg/ml)
Control
rhCSF2
CXCL1 CXCL2 CXCL3 CXCL8
D
IL-6
P=0.0034
CSF2
P=0.0275
CXCL1
P<0.0001
CXCL2
P=0.0003
CXCL3
P=0.0125
CXCL8
P=0.0214
Relative mRNA expression level
Normal Breast cancer-adjacent
E
Relative mRNA expression level
Control
rhCSF2
rhCSF2+Stattic
CXCL1 CXCL2 CXCL3 CXCL8 IL-6 IL-1β
F
rhCSF2:
Stattic:
p-Stat3
Stat3
GAPDH
G
Relative mRNA expression level
Control
Co
Co+α-CSF2
CXCL1 CXCL2 CXCL3 CXCL8
H
Control
Control+α-CSF2
Co
Co+α-CSF2
p-Stat3
Stat3
GAPDH

rhCXCL3 promotes the mesenchymal phenotype, migration, and invasion of breast cancer cells

Recent studies have demonstrated that CXCL3 promotes the migration and invasion of cervical (Qi et al., 2020) and prostate cancer cells (Gui et al., 2016). However, the role of CXCL3 in the progression of breast cancer is unknown. Here, we treated MDA-MB-231 and BT549 cells with rhCXCL3 and found that rhCXCL3 significantly enhanced the migration and invasion of both MDA-MB-231 (Figure 3A and B) and BT549 (Supplementary Figure S3A and B) cells but had no effect on cell proliferation (Supplementary Figure S3C).

Epithelial–mesenchymal transition (EMT) is a process by which epithelial cells acquire a mesenchymal cell phenotype that promotes the invasion and metastasis of tumors (Pastushenko and Blanpain, 2019). In this study, 20 ng/ml rhCXCL3 significantly upregulated the mRNA expression levels of mesenchymal markers, such as N-cadherin, Vimentin, Fibronectin, and α-SMA (Figure 3C and D), and increased the protein expression of N-cadherin and Vimentin (Figure 3E and F) in both MDA-MB-231 and BT549 cells. In addition, TRITC-phalloidin staining showed thicker bundles of F-actin stress fibers in MDA-MB-231 (Figure 3G) and BT549 (Figure 3H) cells, implying that CXCL3 causes the reorganization of the actin cytoskeleton and thus the cells acquire a stronger invasive ability.

The CXCL3/CXCR2 signaling axis activates the FAK signaling pathway to enhance the mesenchymal phenotype of breast cancer cells

FAK plays a crucial role in cell migration and EMT, and the FAK signaling pathway is aberrantly activated in a variety of tumors (Lee et al., 2015; Zhou et al., 2019). FAK phosphorylation is involved in ELR^+ CXC subfamily member-mediated migration, e.g. CXCL1 promotes osteosarcoma metastasis via activating the FAK signaling pathway (Wang et al., 2017). Here, we found that rhCXCL3 treatment increased FAK tyrosine-397 phosphorylation in breast cancer cells (Figure 4A), and the maximum phosphorylation of FAK occurred at 30 min over a 60-min period (Figure 4B).

CSF2 could stimulate adipocytes to secrete various cytokines, including IL-6 and CSF3, that can activate FAK (Li et al., 2022). We found that the combination treatment with CXCL3 and IL-6 or CSF3 further enhanced FAK phosphorylation (Supplementary Figure S3D–G), migration (Supplementary Figure S3H and J), and invasion (Supplementary Figure S3I and K) of MDA-MB-231 cells compared with either treatment alone. These results suggest a potential synergy between CXCL3 and other CSF2-stimulated, CAA-derived secretory factors in the malignant progression of breast cancer.

CXCR2 is a receptor for the CXC subfamily, which plays a critical role in the development of several malignancies. CXCL3 binds to the receptor CXCR2 to promote the metastasis of prostate cancer (Gui et al., 2016; Xin et al., 2018). CXCL3 also binds to CXCR1 to mediate the migration of airway smooth muscle cells (Al-Alwan et al., 2013). However, the role of CXCL3 in breast cancer progression remains unclear. First, we found that the protein expression levels of CXCR1 and CXCR2 were increased in MDA-MB-231, BT549, MCF-7, and T47D cells compared to MCF10A cells (Figure 4C). Next, when treating breast cancer cells with the CXCR1 inhibitor reparixin or the CXCR2 inhibitor SB225002, we found that SB225002, but not reparixin, significantly inhibited rhCXCL3-induced FAK phosphorylation (Figure 4D), suggesting that CXCL3 activates downstream FAK via CXCR2 but not via CXCR1.

To assess whether FAK mediates CXCL3-induced migration and invasion of breast cancer cells, we used PF573228, a FAK tyrosine-397 phosphorylation inhibitor, and found that PF573228 significantly inhibited rhCXCL3-induced migration and invasion of MDA-MB-231 (Figure 4E and F) and BT549 (Supplementary Figure S4A and B) cells and markedly reduced FAK phosphorylation (Figure 4G).

Furthermore, we designed three small interfering RNAs (siRNAs) targeting FAK, among which, #1 and #3 could specifically and effectively silence FAK protein expression in breast cancer MDA-MB-231 cells (Figure 5A). Compared to non-specific siRNAs, siRNAs targeting FAK reduced CXCL3-induced migration (Figure 5B) and invasion (Figure 5C) of breast cancer cells. These results highlight the critical role of FAK signaling in mediating CSF2/CXCL3-induced cancer cell migration and invasion.

Then, breast cancer cells were treated with rhCXCL3 in the presence or absence of PF573228, and the expression levels of mesenchymal markers were examined. The results showed that PF573228 significantly inhibited CXCL3-induced mRNA expression of mesenchymal markers in MDA-MB-231 (Figure 5D) and BT549 (Figure 5E) cells and also potentially inhibited CXCL3-induced protein expression of N-cadherin and Vimentin (Figure 5F), suggesting that CXCL3/CXCR2 signaling activates FAK to promote the mesenchymal phenotype of breast cancer cells.

Figure 2 *(Continued)* CSF2 activates Stat3 to upregulate CXCL3 expression in adipocytes co-cultured with breast cancer cells. (**A**) The mRNA expression levels of CSF2Rα and CSF2Rβ in adipocytes co-cultured with MDA-MB-231 cells were measured by q-PCR. (**B** and **C**) Cytokine expression (**B**) and secretion (**C**) in adipocytes treated with rhCSF2 (20 ng/ml) were detected by q-PCR and ELISA, respectively. (**D**) The mRNA expression levels of IL-6, CSF2, and CXCLs in normal and paracancerous adipose tissues. (**E**) Adipocytes were stimulated with rhCSF2 for 12 h and then treated with stattic (10 μM). The mRNA expression levels of CXCLs, IL-6, and IL-1β in adipocytes were detected. (**F**) Adipocytes were treated with rhCSF2 and stattic for 15 min, and Stat3 phosphorylation was analyzed by western blotting. (**G** and **H**) Adipocytes were co-cultured with MDA-MB-231 cells in the presence or absence of CSF2-neutralizing antibody (2 μg/ml). The expression of CXCLs (**G**) and Stat3 phosphorylation (**H**) in adipocytes were analyzed by q-PCR and western blotting, respectively. $^{###}P < 0.001$, $^{##}P < 0.01$, and $^{#}P < 0.05$ compared to the control group; $^{***}P < 0.001$, $^{**}P < 0.01$, and $^{*}P < 0.05$ compared to experimental group; $n = 3$.

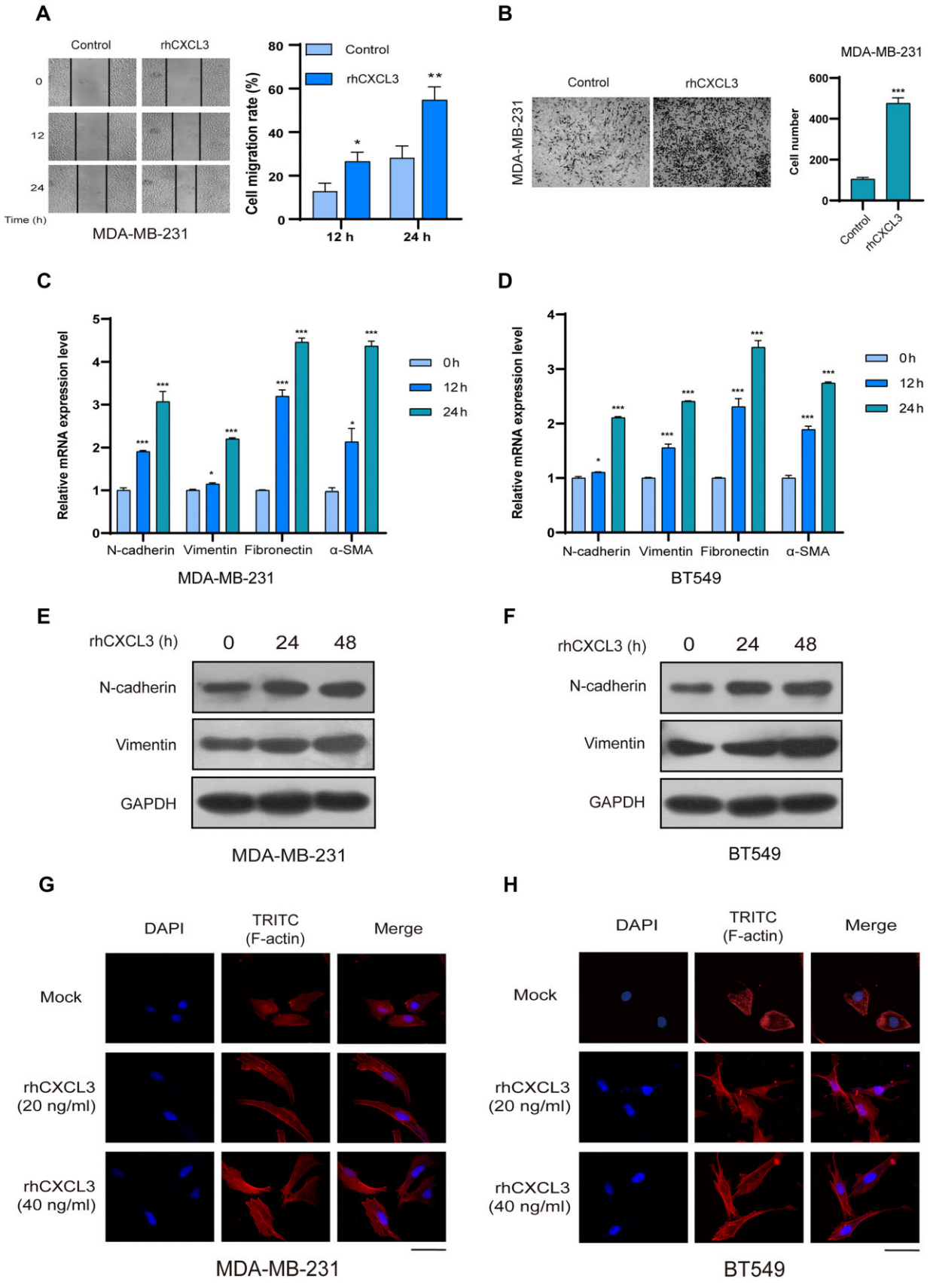
A
Control
rhCXCL3
0
12
24
Time (h)
MDA-MB-231
Cell migration rate (%)
12 h
24 h
B
MDA-MB-231
Control
rhCXCL3
Cell number
C
Relative mRNA expression level
0h
12h
24h
N-cadherin
Vimentin
Fibronectin
α-SMA
MDA-MB-231
D
BT549
E
rhCXCL3 (h)
0
24
48
GAPDH
F
G
DAPI
TRITC (F-actin)
Merge
Mock
rhCXCL3 (20 ng/ml)
rhCXCL3 (40 ng/ml)
H

CXCL3-neutralizing antibody inhibits CAA-promoted migration, invasion, and FAK phosphorylation of breast cancer cells

To determine whether CXCL3 mediates CAA-promoted breast cancer invasion, breast cancer cells were treated with conditioned media from CAAs or mature adipocytes followed by incubation with CXCL3-neutralizing antibody. Both CAA-derived conditioned media (CAA-CM) and mature adipocyte-derived conditioned media (Adi-CM) effectively promoted the migration and invasion of MDA-MB-231 (Figure 6A and B) and BT549 (Supplementary Figure S4C and D) cells, which were significantly inhibited by CXCL3-neutralizing antibody. In addition, CAA-CM and Adi-CM also enhanced FAK phosphorylation in MDA-MB-231 and BT549 cells (Figure 6C), which was significantly inhibited by CXCL3-neutralizing antibody (Figure 6D). These results suggest that CAA- or mature adipocyte-derived CXCL3 promotes the migration and invasion of breast cancer cells and activates FAK signaling in breast cancer cells.

Inhibition of FAK phosphorylation reverses CAA-promoted migration and invasion of breast cancer cells

Breast cancer cells were treated with Adi-CM or CAA-CM in the presence or absence of the FAK inhibitor PF573228. The results showed that PF573228 significantly inhibited CAA-induced migration and invasion of MDA-MB-231 (Figure 6E and F) and BT549 (Supplementary Figure S5A and B) cells and also reduced CAA-induced FAK phosphorylation in MDA-MB-231 (Figure 6G) and BT549 (Figure 6H) cells. Western blotting results showed that the FAK inhibitor was more efficient in CAA-CM-treated cells than in Adi-CM-treated cells (Figure 6G and H), probably due to the stronger activation of the FAK pathway induced by CAA-CM. These results suggest that adipocyte-derived CXCL3 promotes the migration and invasion of breast cancer cells via FAK signaling.

CSF2 upregulates CXCL3 expression in adipocytes to promote the migration and invasion of breast cancer via FAK signaling

To explore the role of CSF2 in breast cancer metastasis, breast cancer cells were treated with CAA-CM in the presence or absence of CSF2-neutralizing antibody. As shown in Figure 7A and B, CSF2-neutralizing antibody significantly inhibited CAA-CM-induced FAK phosphorylation in MDA-MB-231 and BT549 cells.

Next, breast cancer cells were treated with the CSF2-stimulated adipocyte culture supernatant (CSF2-CM) in the presence or absence of CXCL3-neutralizing antibody or SB225002. The results showed that CXCL3-neutralizing antibody or SB225002 effectively inhibited CSF2-CM-induced migration and invasion of MDA-MB-231 (Figure 7C and D) and BT549 (Supplementary Figure S5C and D) cells and also inhibited CSF2-CM-induced FAK phosphorylation in MDA-MB-231 (Figure 7E) and BT549 (Figure 7F) cells. These results suggest that CSF2 activates FAK signaling to promote breast cancer cell migration and invasion via upregulation of CXCL3.

High expression of CSF2 and CXCL3 in adipocytes adjacent to breast cancer

Hematoxylin and eosin (H&E) staining and immunohistochemistry (IHC) results showed that the levels of CSF2, CXCL3, and FAK phosphorylation were low in normal mammary tissues but significantly increased in breast cancer tissues (Figure 7G and I). Notably, CSF2 and CXCL3 were highly expressed in paracancerous adipose tissues (Figure 7H). These results confirm that FAK signaling in breast cancer cells is significantly activated and positively correlated with the high expression of CSF2 and CXCL3 in adjacent adipose tissues.

Targeting CSF2 and CXCR2 shows a synergistic inhibition on adipocyte-induced lung metastasis of breast cancer cells in mice

Mouse 4T1 breast cancer cells were co-cultured with mature 3T3-L1 adipocytes. q-PCR results showed that the expression levels of differentiation markers of adipocytes, including PPAR-γ and C/EBP-α, in 3T3-L1 cells were significantly downregulated, whereas that of the cytokines IL-6, CSF2, CXCL1, CXCL2, and CXCL3 were substantially upregulated (Supplementary Figure S6A). In addition, Stat3 was activated in 3T3-L1 cells (Supplementary Figure S6B), implying that 4T1 cells induce 3T3-L1 cells to differentiate into CAAs after co-culture. FAK phosphorylation was also enhanced in 4T1 cells co-cultured with 3T3-L1 cells for 24 h (Supplementary Figure S6C). Thus, mouse breast cancer cells could promote the transformation of 3T3-L1 adipocytes into CAAs via Stat3, leading to the secretion of inflammatory factors.

To establish a mouse model of adipocyte-induced breast cancer lung metastasis, 4T1 cells co-cultured with 3T3-L1 adipocytes were treated without or with CSF2-neutralizing antibody and/or SB225002 for 3 days and then injected into mice via the tail vein. The lung metastasis of breast cancer cells was examined after two weeks (Figure 8A). As shown in Figure 8B–D, the number and size of metastatic lung nodules were significantly increased in the co-culture group compared to the control group (4T1 cells alone), which were reduced after treated with CSF2-neutralizing antibody or SB225002 alone.

Figure 3 *(Continued)* rhCXCL3 promotes the mesenchymal phenotype, migration, and invasion of breast cancer cells. (**A** and **B**) MDA-MB-231 cells were treated with rhCXCL3 (20 ng/ml). Cell migration and invasion were measured by the wound-healing assay (**A**) and the Transwell invasion assay (**B**), respectively. (**C** and **D**) MDA-MB-231 (**C**) and BT549 (**D**) cells were treated with rhCXCL3 for 12 and 24 h, and the mRNA expression levels of EMT markers were detected by q-PCR. (**E** and **F**) MDA-MB-231 (**E**) and BT549 (**F**) cells were treated with rhCXCL3 for 24 and 48 h, and the protein expression levels of N-cadherin and Vimentin were detected by western blotting. (**G** and **H**) MDA-MB-231 (**G**) and BT549 (**H**) cells were treated with 20 and 40 ng/ml rhCXCL3 for 24 h, and the cytoskeleton was stained with TRITC-phalloidin. Scale bar, 20 μm. $^{***}P < 0.001$, $^{**}P < 0.01$, and $^{*}P < 0.05$; $n = 3$.

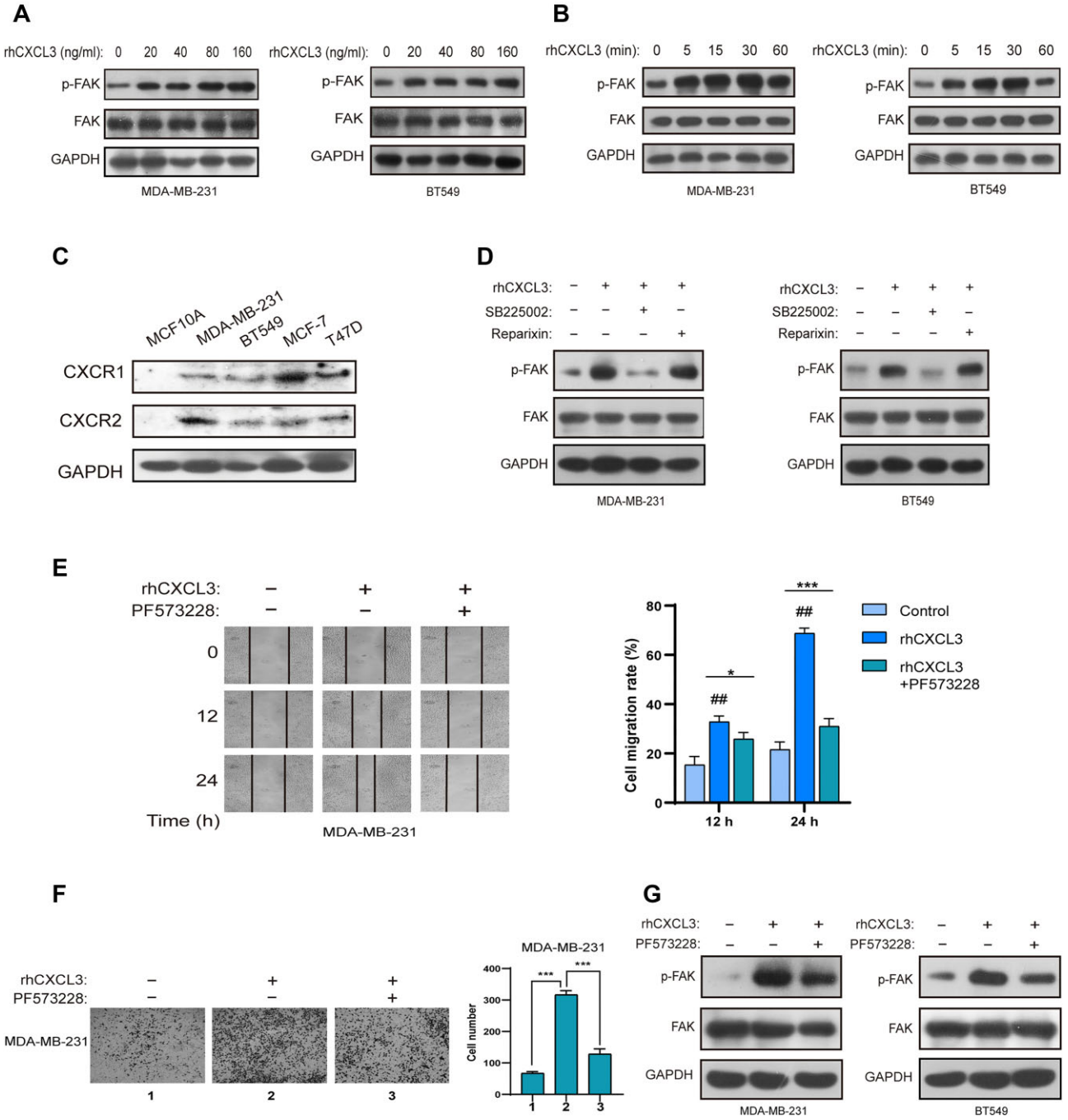

Figure 4 CXCL3/CXCR2 signaling activates FAK to enhance the mesenchymal phenotype of breast cancer cells. (**A**) MDA-MB-231 and BT549 cells were treated with rhCXCL3 at doses of 20, 40, 80, and 160 ng/ml for 30 min. FAK phosphorylation was analyzed by western blotting. (**B**) Breast cancer cells were treated with 20 ng/ml rhCXCL3 for 5, 15, 30, and 60 min, and FAK phosphorylation was analyzed. (**C**) The protein expression levels of CXCR1 and CXCR2 in MCF10A, MBA-MB-231, BT549, MCF-7, and T47D cells. (**D**) MDA-MB-231 and BT549 cells were treated with rhCXCL3 in the presence or absence of SB225002 (0.1 μM) or reparixin (0.1 μM), and FAK phosphorylation was analyzed. (**E** and **F**) MDA-MB-231 cells were treated with rhCXCL3 and/or PF573228 (5 μM). Cell migration (**E**) and invasion (**F**) were measured. (**G**) MDA-MB-231 and BT549 cells were treated with rhCXCL3 and/or PF573228 for 30 min. FAK phosphorylation was analyzed. $^{\#\#\#}P < 0.001$, $^{\#\#}P < 0.01$, and $^{\#}P < 0.05$ compared to the control group; $^{***}P < 0.001$, $^{**}P < 0.01$, and $^{*}P < 0.05$ compared to the experimental group; $n = 3$.

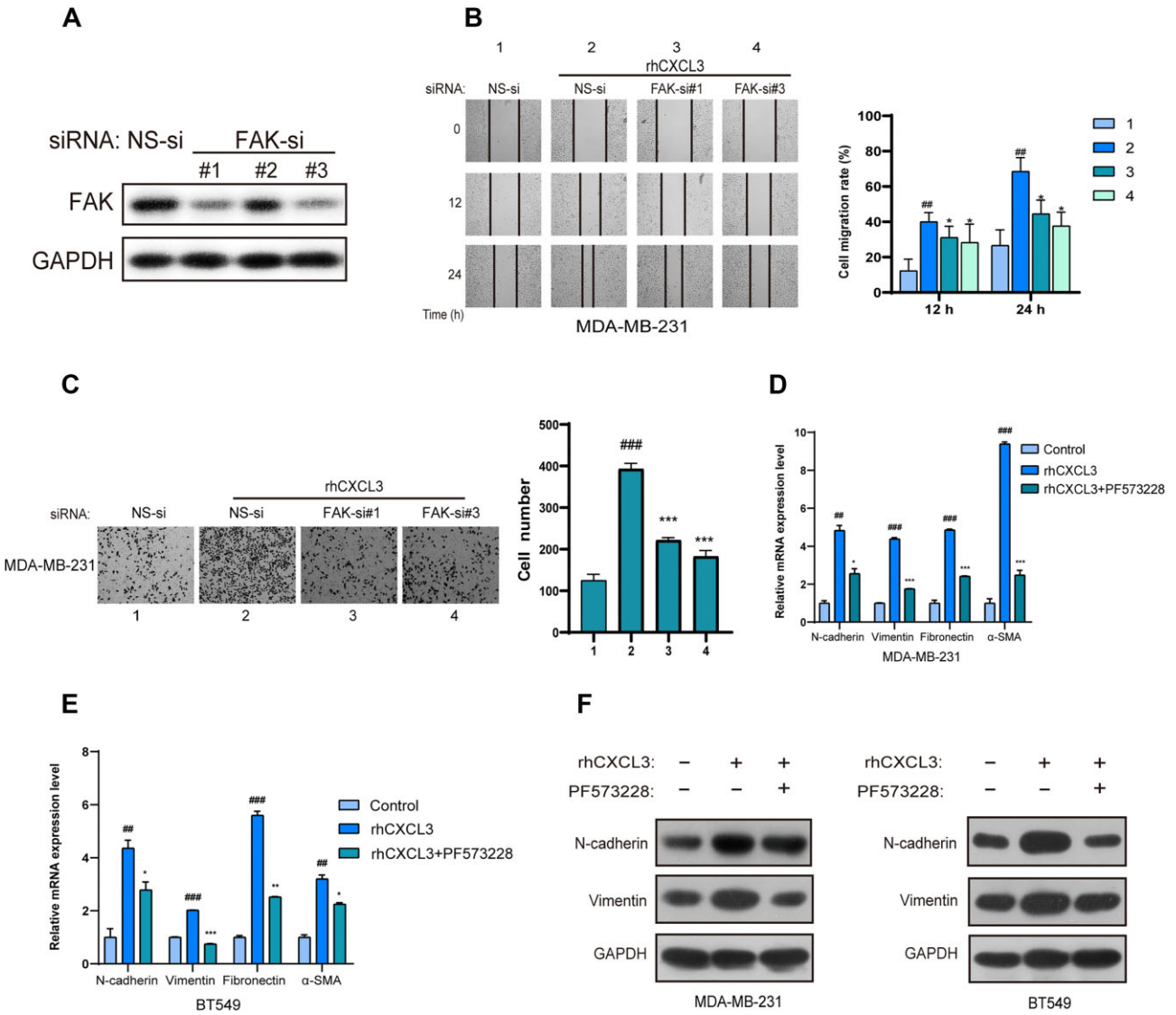

Figure 5 Downregulation of FAK inhibits CXCL3-induced migration and invasion of breast cancer cells. (**A**) FAK protein levels in MDA-MB-231 cells transfected with siRNAs were measured by western blotting. (**B** and **C**) MDA-MB-231 cells transfected with siRNAs were treated with rhCXCL3. Cell migration (**B**) and invasion (**C**) were measured. (**D** and **E**) MDA-MB-231 (**D**) and BT549 (**E**) cells were treated with rhCXCL3 and/or PF573228, and the mRNA expression levels of EMT markers were detected by q-PCR. (**F**) MDA-MB-231 and BT549 cells were treated with rhCXCL3 and/or PF573228, and the protein expression levels of N-cadherin and Vimentin were detected by western blotting. $^{###}P < 0.001$, $^{##}P < 0.01$, and $^{#}P < 0.05$ compared to the control group; $^{***}P < 0.001$, $^{**}P < 0.01$, and $^{*}P < 0.05$ compared to the experimental group; $n = 3$.

The combination treatment with CSF2-neutralizing antibody and SB225002 showed a synergistic effect on lung metastasis, characterized by the remarkable reduction of metastatic nodules compared to co-culture groups.

Discussion

In the early stage of breast cancer, local cancer cells invade adipose tissue. Cancer cells induce adipocyte metabolic reprogramming through constant dynamic interactions with adipocytes, and then adipocytes are activated and transformed into CAAs (Dirat et al., 2011; Wu et al., 2019). However, the molecular mechanism of CAA generation remains unclear. This study demonstrates that CSF2 is highly expressed and secreted by cancer cells and adipocytes in the breast cancer microenvironment. Previous studies showed that preadipocytes promote tumor progression (Reggiani et al., 2017; Kim et al., 2018). CSF2 is highly expressed in both preadipocytes and adipocytes co-cultured with breast cancer cells, but CSF2 expression level in preadipocytes is lower than that in mature adipocytes, suggesting that CSF2 in mature adipocytes in the tumor microenvironment may play a more important role in promoting tumor progression.

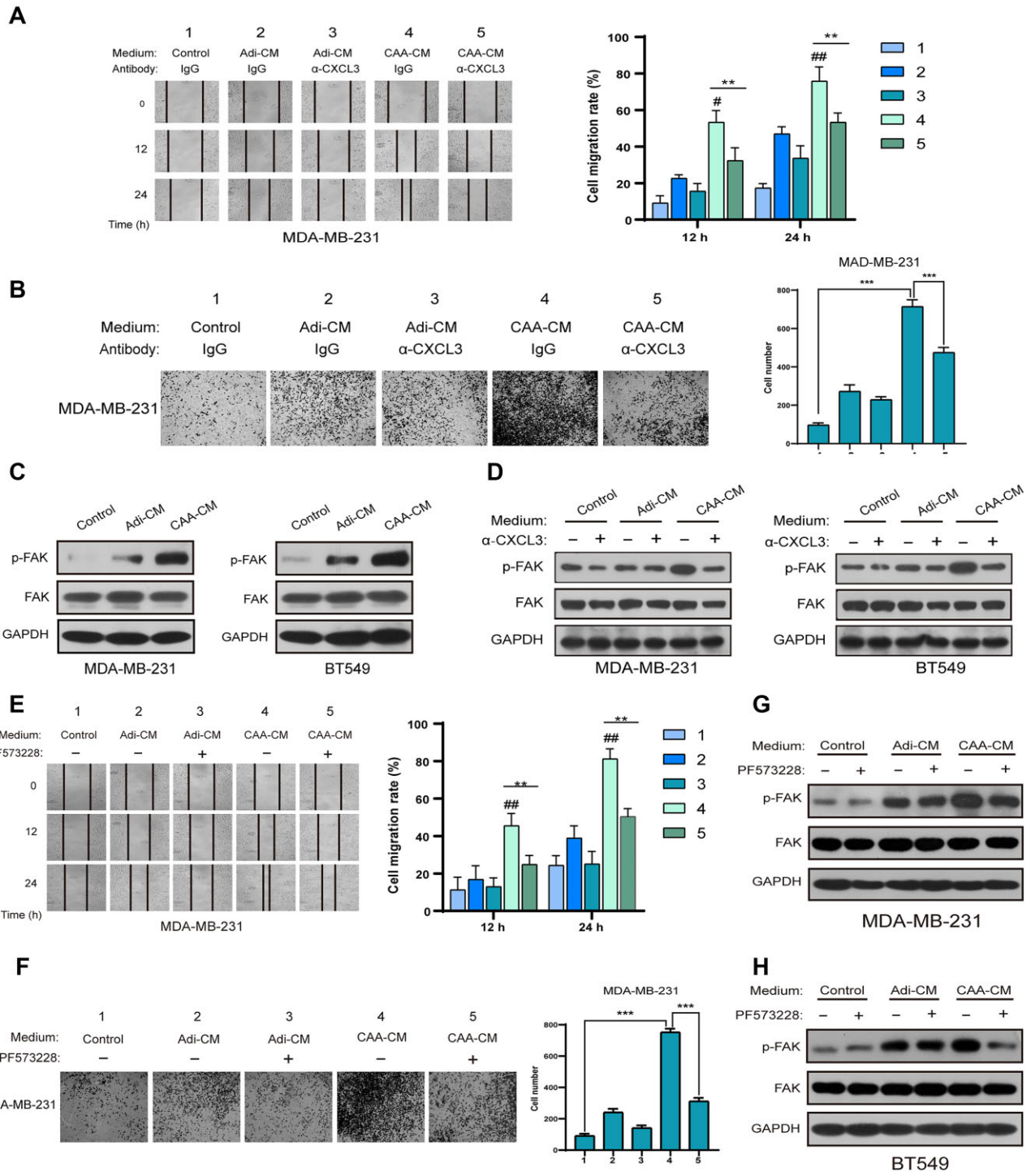

Figure 6 Both CXCL3-neutralizing antibody and PF573228 inhibit CAA-CM-promoted migration, invasion, and FAK phosphorylation of breast cancer cells. (**A** and **B**) MDA-MB-231 cells treated with Adi-CM, CAA-CM, or control medium were incubated with CXCL3-neutralizing antibody (2 μg/ml) or its IgG control. Cell migration (**A**) and invasion (**B**) were measured. (**C**) MDA-MB-231 and BT549 cells were treated with Adi-CM, CAA-CM, or control medium for 30 min. FAK phosphorylation was measured by western blotting. (**D**) MDA-MB-231 and BT549 cells treated with Adi-CM or CAA-CM were cultured with or without CXCL3-neutralizing antibody. FAK phosphorylation was analyzed. (**E** and **F**) MDA-MB-231 cells treated with Adi-CM or CAA-CM were incubated with or without PF573228, and cell migration (**E**) and invasion (**F**) were measured. (**G** and **H**) MDA-MB-231 (**G**) and BT549 (**H**) cells were treated with Adi-CM or CAA-CM for 30 min, with or without PF573228. FAK phosphorylation was analyzed. $^{###}P < 0.001$, $^{##}P < 0.01$, and $^{#}P < 0.05$ compared to the control group; $^{***}P < 0.001$, $^{**}P < 0.01$, and $^{*}P < 0.05$ compared to the experimental group; $n = 3$.

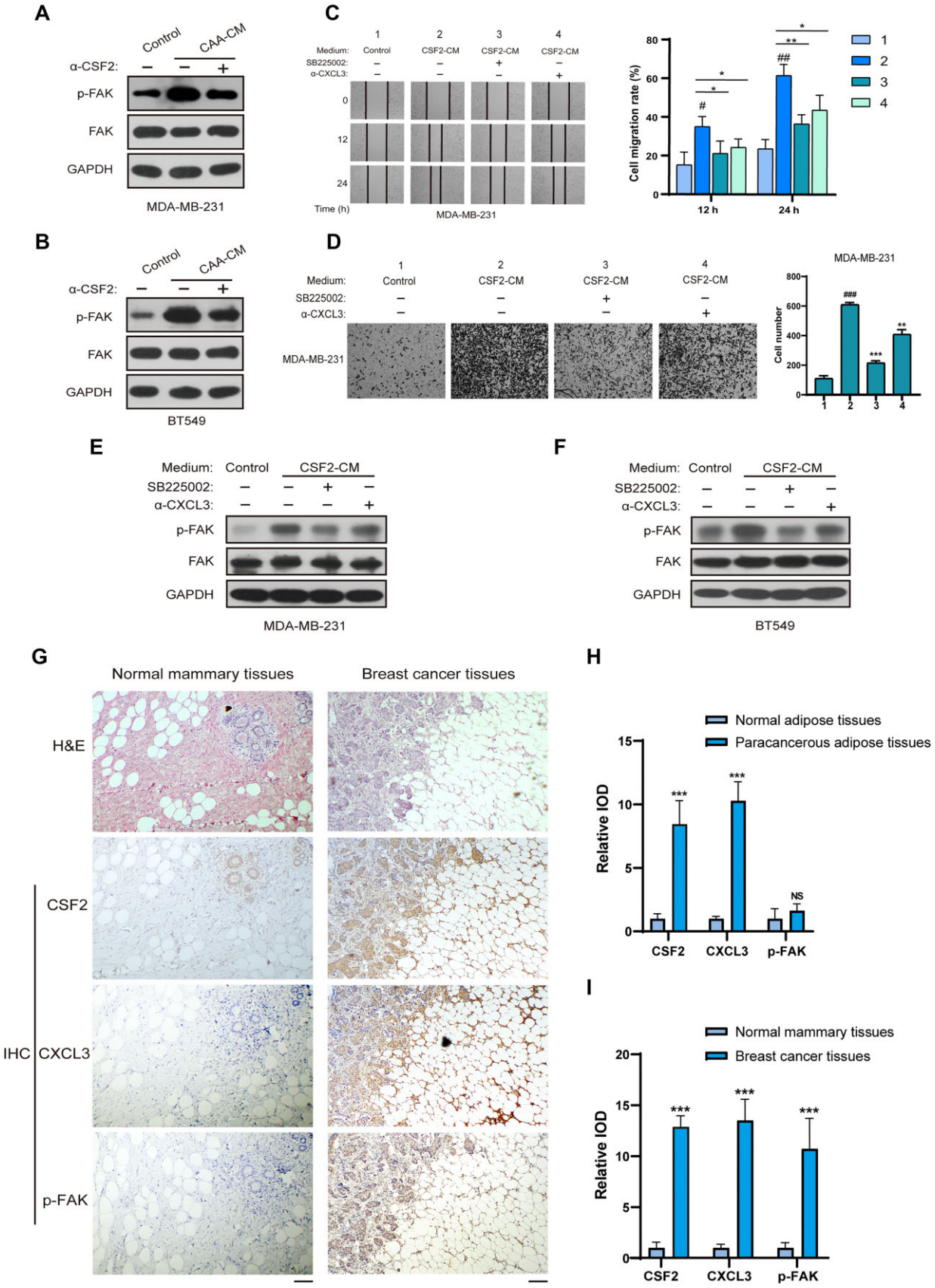
A
Control
CAA-CM
α-CSF2:
p-FAK
FAK
GAPDH
MDA-MB-231
B
BT549
C
Medium:
SB225002:
α-CXCL3:
Time (h)
Cell migration rate (%)
12 h
24 h
D
Cell number
E
F
G
Normal mammary tissues
Breast cancer tissues
H&E
CSF2
CXCL3
p-FAK
IHC
H
Normal adipose tissues
Paracancerous adipose tissues
Relative IOD
NS
I

CSF2 is overexpressed in various tumors. It exerts pro-tumorigenic effects by promoting the proliferation, migration, and invasion of cancer cells and upregulating anti-apoptotic and pro-angiogenic signaling (Jung et al., 2006; Revoltella et al., 2012; Hong, 2016). However, the biological effects of CSF2 on adipocytes were barely explored. In CSF2 knockout mice, the expression levels of inflammatory factors IL-1β, TNF-α, and MIP1α are significantly reduced in the mesenteric adipose (Kim et al., 2008), suggesting that CSF2 may be involved in the inflammatory phenotype of CAAs. In this study, we found that CSF2 upregulates the expression of multiple inflammatory factors such as IL-6, IL-1β, CCL2, CXCL1, CXCL2, CXCL3, and CXCL8 in adipocytes via activating the Stat3 signaling pathway, suggesting that the CSF2/Stat3 pathway may play a crucial role in the generation of CAA inflammatory phenotype.

CXCL3, also known as growth regulatory oncogene gamma, belongs to the ELR^+ CXC subfamily of the chemokine CXC family. Recent studies showed that CXCL3 is overexpressed in tumors (Reyes et al., 2021). CXCL3 also promotes the proliferation and migration of cervical cancer, lung cancer, and oral squamous cell carcinoma cells via the MAPK/ERK signaling pathway (Zhang et al., 2016; Qi et al., 2020; Weng et al., 2021). Although CXCL3 has been found highly expressed in breast cancer (See et al., 2014), the cell source of CXCL3 and its role in the development of breast cancer are not disclosed. Our study demonstrates that CXCL3 promotes the mesenchymal phenotype, migration, and invasion of breast cancer cells. The inhibition of CXCL3 suppresses CAA-CM-induced migration and invasion of breast cancer cells, suggesting that CAA-promoted tumor aggressiveness is mediated by adipocyte-derived CXCL3.

To investigate the molecular mechanism of CXCL3-induced EMT in breast cancer cells, we examined the downstream molecules of CXCL3. We found that CXCL3 targets the breast cancer surface receptor CXCR2 to activate the FAK pathway. FAK is at the intersection of various signaling pathways that promote tumor growth and metastasis, and its tyrosine kinase activity is regulated by integrins. Integrins mediate bidirectional signaling inside and outside the cells (Pang et al., 2023). Integrin/FAK signaling could be activated by chemokines, thus transmitting signals between cells and ECM. Previous studies showed that CXCL8/CXCR2-activated FAK phosphorylation is adhesion-dependent and requires stimulation of the ECM protein Fibronectin (Cohen-Hillel et al., 2006). In addition, CXCL8/CXCR2 can activate FAK/paxillin via β1-integrin/Fibronectin (Cohen-Hillel et al., 2009). Therefore, CXCL3/CXCR2 signaling in breast cancer cells activates integrin/FAK signaling probably by activating the cytoplasmic region of β1-integrin, which could transmit signals from the inside of the cell to the outside and *vice versa*. FAK may further activate signaling pathways such as p130Cas/Cas/Crk, PI3K/AKT, and MAPK to induce EMT (Chuang et al., 2022).

Inhibition of FAK or CXCL3 suppresses CXCL3- or CAA-induced migration and invasion of breast cancer cells, implying that adipocyte-derived CXCL3 activates FAK signaling to promote breast cancer aggressiveness. In addition, CSF2-CM significantly promotes FAK phosphorylation, migration, and invasion of breast cancer cells, which are blocked by inhibition of CXCL3 or CXCR2. Taken together, these data indicate that CSF2 activates FAK signaling via upregulating CXCL3 expression in adipocytes. Our *in vivo* study further demonstrates that inhibition of CSF2 in the co-culture system and inhibition of CXCR2 signaling in breast cancer cells synergistically diminish adipocyte-induced lung metastasis of breast cancer cells, suggesting a potential of co-targeting CSF2 and CXCR2 for alleviating breast cancer metastasis.

Overweight and obesity increase breast cancer incidence and mortality rates, especially among postmenopausal women (Lauby-Secretan et al., 2016). In obese individuals, the significant increase in the number and size of adipocytes leads to adipose tissue dysfunction, characterized by chronic inflammation and abnormal cytokine and hormone secretion, which could promote tumorigenesis and malignant progression. Similar to CAAs, adipocytes in obese patients secrete multiple pro-inflammatory cytokines, such as IL-6, CCL2, VEGF, Leptin, etc. (Picon-Ruiz et al., 2017). However, whether adipocyte dysfunction promotes obesity-associated cancer via CSF2 or CXCL3 needs to be investigated.

In summary, our study revealed that breast cancer cell- and adipocyte-secreted CSF2 could activate the Stat3 pathway in CAAs in the paracrine or autocrine manner, leading to the increased expression and secretion of CXCL3. CXCL3 binds to CXCR2, a receptor on breast cancer cells, and activates FAK, which promotes the mesenchymal phenotype, invasion, and metastasis of breast cancer cells (Figure 8E). These findings highlight the importance of the CSF2/CXCL3/FAK axis in breast cancer metastasis. Co-targeting CSF2 and CXCR2 abrogates lung metastasis of breast cancer cells in a mouse model, thus representing a novel therapeutic strategy for breast cancer metastasis.

Figure 7 *(Continued)* CSF2 upregulates CXCL3 expression in adipocytes to promote the migration and invasion of breast cancer cells via FAK signaling. (**A** and **B**) MDA-MB-231 (**A**) and BT549 (**B**) cells were cultured with CAA-CM in the presence or absence of CSF2-neutralizing antibody for 30 min. FAK phosphorylation was analyzed by western blotting. (**C** and **D**) MDA-MB-231 cells were incubated with CSF2-CM followed by treatment with SB225002 or CXCL3-neutralizing antibody. The migration (**C**) and invasion (**D**) were measured. (**E** and **F**) MDA-MB-231 (**E**) and BT549 (**F**) cells were treated with CSF2-CM followed by incubation with SB225002 or CXCL3-neutralizing antibody for 30 min. FAK phosphorylation was analyzed. (**G**) H&E staining and IHC images showing the expression of CSF2, CXCL3, and p-FAK in normal mammary and breast cancer tissues. Scale bar, 200 μm. (**H** and **I**) IHC images were analyzed with Image-ProPlus, and the relative integral optic density (IOD) of each group was calculated to indicate the protein expression level ($n = 10$). $^{###}P < 0.001$, $^{##}P < 0.01$, and $^{#}P < 0.05$ compared to the control group; $^{***}P < 0.001$, $^{**}P < 0.01$, and $^{*}P < 0.05$ compared to the experimental group; $n = 3$.

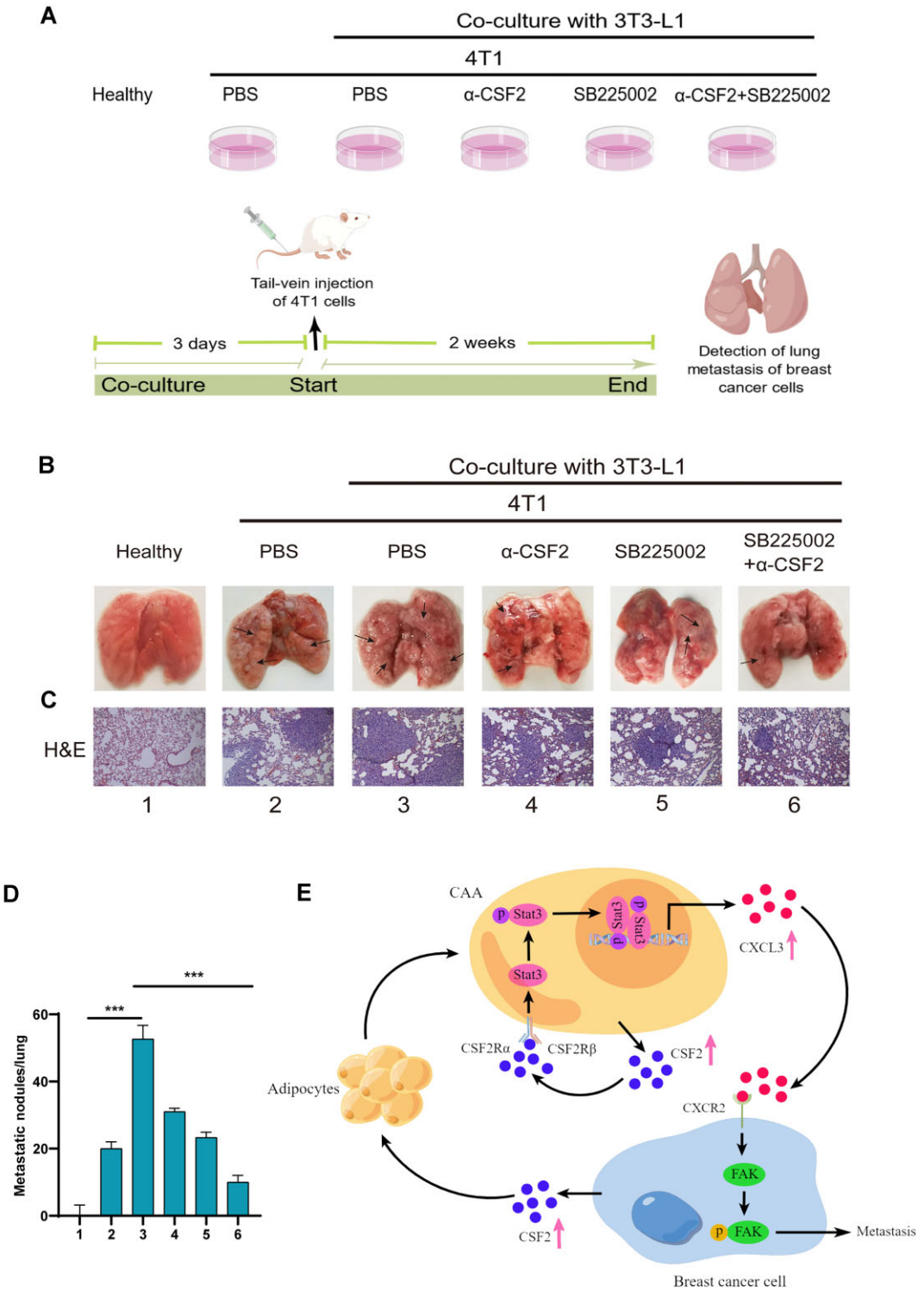

Figure 8 CSF2-neutralizing antibody and CXCR2 inhibitor synergistically inhibit adipocyte-induced lung metastasis of breast cancer cells in mice. (**A**) Schematic diagram presenting the development of lung metastasis of breast cancer cells in a mouse model, by Figdraw (www.figdraw.com accessed on April 6, 2023). (**B** and **C**) Representative photos (**B**) and H&E staining images (**C**) of the lungs from healthy and 4T1 cell-bearing mice. Black arrows indicate typical metastatic lung nodules. (**D**) Quantification of metastatic nodules in mouse lungs of each group. (**E**) Schematic diagram showing the role of the CSF2/CXCL3/FAK signaling axis in promoting breast cancer metastasis, by Figdraw (www.figdraw.com accessed on July 29, 2022). ***$P < 0.001$, **$P < 0.01$, and *$P < 0.05$; $n = 6$.

Materials and methods

Cytokines and inhibitors

Recombinant human CSF2 (#300-03), CSF3 (#300-23), CXCL3 (#300-40), and IL-6 (#200-06) were purchased from PeproTech. CSF2-neutralizing antibody (#ab9741) was purchased from Abcam. CXCL3-neutralizing antibody (PP1014P2) was purchased from Origene. SB225002 (#HY-16711), reparixin (#HY-15251), and stattic (#HY-13818) were purchased from Med Chem Express. PF573228 (#M2931) was purchased from Abmole.

Antibodies

Antibodies against Stat3 (#9139; 1:500) and pY705-Stat3 (#9145; 1:1000) were purchased from Cell Signaling Technology. Anti-FAK (#T55464; 1:1000) and anti-pTyr397-FAK (#T55587; 1:2000) antibodies were purchased from Abmart. Anti-N-cadherin (#66219-1-Ig; 1:3000), anti-Vimentin (#60330-1-Ig; 1:3000), and anti-GAPDH (#60004-1-Ig; 1:5000) antibodies were purchased from Proteintech. Anti-CXCR1(#YT6039; 1:1000), anti-CXCR2 (#YT5397; 1:1000), anti-CXCL3 (#YT2075; IHC, 1:100), and anti-FAK p-Tyr397 (#YP0739; IHC, 1:100) antibodies were purchased from Immunoway.

Patient specimens

Human breast cancer and adjacent normal mammary tissues were obtained from breast cancer patients who underwent lumpectomy. All patients signed the informed consent form for inclusion in the research project. This study was conducted in accordance with the Declaration of Helsinki and approved by the Ethics Committee of Jiangxi Cancer Hospital (Approval No.: 2020ky164).

Cell culture

Human triple-negative breast cancer cell lines MDA-MB-231 and BT549, estrogen receptor-positive breast cancer cell line MCF-7, estrogen receptor-positive human breast ductal carcinoma cell line T47D, and human normal mammary epithelial cell line MCF10A were purchased from Procell Life Science & Technology Co., Ltd. Mouse breast cancer cell line 4T1 and preadipocyte cell line 3T3-L1 were purchased from the Cell Bank of Type Culture Collection of Chinese Academy of Sciences. MDA-MB-231, MCF-7, T47D, and 4T1 cells were maintained in Dulbecco's modified Eagle's medium (DMEM) containing 10% fetal bovine serum (FBS) (#10099141C, Gibco). BT549 and 4T1 cells were maintained in RPMI 1640 medium containing 10% FBS. MCF10A cells were maintained in MCF10A-specific medium (#CM-0525, Procell).

Primary culture of human preadipocytes

Fresh adipose tissue from the excised human breast was collected aseptically and washed with phosphate-buffered saline (PBS) to remove blood cells. The yellow adipose tissue was separated and minced, incubated with an equal volume of 0.1% collagenase I (#C8140, Solarbio) at 37°C for 1 h, and then filtrated through a 100-μm mesh sieve to remove adipose tissue debris. The filtrate was centrifuged at 2000 rpm for 5 min. The sediment containing the stromal vascular fraction was washed twice with PBS, and the cells were resuspended in DMEM/F12 medium containing 10% FBS and incubated at 37°C with 5% CO_2 (Zhou et al., 2022).

Induced differentiation of preadipocytes and 3T3-L1 cells

Preadipocytes were maintained in differentiation-inducing A solution containing IBMX (0.5 mM, #28822-58-4, Sigma), dexamethasone (0.5 μM, #50-02-2, Sigma), rosiglitazone (2 μM, #122320-73-4, Sigma), and insulin (5 μg/ml, #11061-68-0, Sigma). After 3 days, the medium was changed with a differentiation-inducing B solution containing insulin (5 μg/ml) to continue inducing differentiation for another day. The differentiation induction was completed after 12–16 days by alternative culture with A and B solutions. 3T3-L1 cells were maintained in a differentiation-inducing A solution containing dexamethasone (0.5 μM), insulin (5 μg/ml), and IBMX (0.5 mM) for 2 days. The medium was then changed with a differentiation-inducing B solution containing insulin (5 μg/ml), and differentiation was completed after 4 days.

Cell co-culture and CM production

Breast cancer cells and adipocytes/CAAs were co-cultured in the Transwell chamber with a pore size of 0.4 μm (#3415, Corning). The breast cancer cells were seeded in the upper layer, and adipocytes were cultured in the lower layer. After 24 h of co-culture, the chamber was removed, the culture was continued using serum-free DMEM, and the adipocyte supernatant was collected after 24 h and stored at −80°C.

Total RNA extraction and real-time q-PCR

Paracancerous adipose tissue surrounding 0.5 cm of breast cancer tissue was harvested. Tissues were then well ground on ice with a grinding rod. Total RNA from tissues was isolated using TRIzol (#T9108, TaKaRa) according to the manufacturer's instructions. Then, 1 μg of RNA was reverse-transcribed using the ReverTra Ace® q-PCR RT kit (#FSQ-101, TOYOBO), and q-PCR was performed using the SYBR® Premix Ex TaqTM kit (#DRR820A, TaKaRa) on an ABI7500 Real-Time PCR System (Applied Biosystems). Gene expression levels were normalized by S18 for adipocytes/adipose tissue and GAPDH for breast cancer cells/breast cancer tissue. The primers are listed in Supplementary Table S2.

ELISA

CSF2, CXCL1, CXCL2, CXCL3, and CXCL8 in conditioned culture supernatant of adipocytes or tumor cells were measured using ELISA kits (#EK163, #EK196, #EK1264, #EK1265, #EK108, MultiSciences). The samples were added to the wells of the ELISA plate and incubated with the detection antibody for 2 h at room temperature, followed by 100 μl of horseradish peroxidase-labeled streptavidin per well for 30 min and then 100 μl of the chromogenic substrate TMB per well for 30 min. The absorbances at 450 nm and 570 nm were measured

immediately using a SpectraMax® Paradigm® Microplate Reader (Molecular Devices).

Western blotting

Cells were treated with lysis buffer containing protease inhibitor, then lysed at 4°C for 30 min, and centrifuged at 12000 rpm for 15 min. The protein sample was diluted by adding loading buffer and denatured at 100°C. Equal amounts of protein samples were added to a polyacrylamide gel and electrophoresed at 80 V. The proteins were transferred to nitrocellulose at 200 mA and then blocked with 5% skim milk for 1 h, followed by incubation with the primary antibody overnight and then the secondary antibody for 4 h at 4°C. The signal was detected using the ECL Prime Western Blotting Detection Reagent.

Wound-healing assay

Cells were seeded in 12-well plates for 24 h, and then three parallel lines were drawn equidistantly. Stimulating factors and 0.2% FBS were added to DMEM. Cells were photographed and recorded every 12 h using a phase-contrast microscope to evaluate cell migration.

Transwell invasion assay

The bottom of the 24-well Transwell chamber with a pore size of 8 μm (#3422, Corning) was coated with Matrigel (#354234, Corning). Cells (1×10^5) were cultured the Transwell chamber, and the culture medium or recombinant protein was added to the outer chamber. After 24 h of culture, the cells on the outside bottom of the Transwell chamber were fixed with 4% paraformaldehyde and stained with 0.1% crystal violet solution for 20 min. The chambers were rinsed with PBS and air-dried, and the invaded cells were observed under a microscope. Five randomly selected fields of view were photographed and examined.

MTT assay

Approximately 5×10^3 cells were cultured in each well of 96-well plates for 24 h. Culture medium was replaced with serum-free medium. The stimulating factor was added to the experimental group. After 48 h, the supernatant was aspirated, and 100 μl DMSO was added to each well. Cell proliferation was determined by measuring the absorbance at 450 nm. Data are expressed as the absorbance value of the experimental group after subtraction of the control group.

siRNA transfection

Cells were replaced with new Opti-MEM 2 h before transfection. The siRNA (RiboBio) was diluted with Opti-MEM to the final concentration of 50 nM and then mixed with TurboFect Transfer Agent (R0531, Thermo Fisher) by gentle inversion. After 20 min incubation at room temperature, the mixed solution was added to the cells. The medium was replaced with complete medium after 12 h, and samples were harvested to test the transfection efficiency or to conduct subsequent experiments after 48 h. The following FAK-specific siRNA sequences are used: #1, 5′-ACACCAAATTCGAGTACTA-3′; #2, 5′-CCCTAACCATTGCGGAG AA-3′; and #3, 5′-CCACCTGGGCCAGTATTAT-3′.

TRITC-phalloidin staining

Breast cancer cells were seeded on coverslips in 24-well plates and cultured in serum-free DMEM containing stimulating factors. After 24–48 h, the cells were fixed with 4% paraformaldehyde at room temperature for 10 min, permeabilized with 0.5% Triton X-100 solution for 5 min, then incubated with 100 nM TRITC-phalloidin (MF8024, MesGenBiotech) in the dark for 20 min, and observed under a confocal microscope.

Tail-vein metastasis assay

Six-week-old female BALB/c SPF mice were purchased from Hunan SJA Laboratory Animal Co., Ltd. Mouse 3T3-L1 preadipocytes were differentiated into mature adipocytes and then co-cultured with 4T1 cells in the presence or absence of CSF2-neutralizing antibody and/or SB22500 for 3 days. The harvested 4T1 cells (1×10^6 cells per mouse) were injected into mice via the tail vein. After 2 weeks, the mice were euthanized, and lung tissues were harvested for analysis. All procedures were approved by the Animal Research Ethics Committee of Nanchang University (Approval No.: NDSYDWLL-2020089).

H&E staining and IHC

Fresh mouse lung tissues were fixed in tissue fixation solution for 12 h and then dehydrated in different gradients of alcohol. The tissues were embedded in paraffin wax, and the paraffin blocks were cut into 5 μm slices and attached to slides for drying. The sections were dewaxed in xylene and hydrated in different gradients of alcohol followed by staining with a hematoxylin solution, differentiating and converting to a blue color. The sections were then stained with an eosin solution, dehydrated, cleared, and mounted with neutral resin.

For IHC, human breast cancer tissue sections were incubated in 3% H_2O_2 for 10 min after deparaffinization and hydration. After washing with PBS extensively, the sections were incubated in goat serum for 30 min, then stained with anti-CSF2, anti-CXCL3, and anti-p-FAK at 4°C overnight, and subsequently incubated with secondary IgG for 1 h. Peroxidase activity was observed with a diaminobenzidine tetrachloride solution.

Statistical analysis

Statistical analysis was performed using GraphPad Prism statistical software, and data are expressed as mean ± standard deviation. Student's *t*-test was used to compare two groups of samples, and one-way ANOVA was used to compare multiple groups of samples. $P < 0.05$ was considered statistically significant.

Supplementary material

Supplementary material is available at *Journal of Molecular Cell Biology* online.

Funding

This work was supported by grants from the National Natural Science Foundation of China (NSFC) (82260531 and 81760509) and the Natural Science Foundation of Jiangxi Province of China (20181BAB205043 and 20224BAB206057) to X.X.

Conflict of interest: none declared.

References

Al-Alwan, L.A., Chang, Y., Mogas, A., et al. (2013). Differential roles of CXCL2 and CXCL3 and their receptors in regulating normal and asthmatic airway smooth muscle cell migration. J. Immunol. *191*, 2731–2741.

Al-Khalaf, H.H., Al-Harbi, B., Al-Sayed, A., et al. (2019). Interleukin-8 activates breast cancer-associated adipocytes and promotes their angiogenesis- and tumorigenesis-promoting effects. Mol. Cell. Biol. *39*, e00332-18.

Anderson, N.M., and Simon, M.C. (2020). The tumor microenvironment. Curr. Biol. *30*, R921–R925.

Boyer, S., Lee, H.J., Steele, N., et al. (2022). Multiomic characterization of pancreatic cancer-associated macrophage polarization reveals deregulated metabolic programs driven by the GM-CSF–PI3K pathway. eLife *11*, e73796.

Chuang, H.H., Zhen, Y.Y., Tsai, Y.C., et al. (2022). FAK in cancer: from mechanisms to therapeutic strategies. Int. J. Mol. Sci. *23*, 1726.

Cohen-Hillel, E., Mintz, R., Meshel, T., et al. (2009). Cell migration to the chemokine CXCL8: paxillin is activated and regulates adhesion and cell motility. Cell. Mol. Life Sci. *66*, 884–899.

Cohen-Hillel, E., Yron, I., Meshel, T., et al. (2006). CXCL8-induced FAK phosphorylation via CXCR1 and CXCR2: cytoskeleton- and integrin-related mechanisms converge with FAK regulatory pathways in a receptor-specific manner. Cytokine *33*, 1–16.

Dirat, B., Bochet, L., Dabek, M., et al. (2011). Cancer-associated adipocytes exhibit an activated phenotype and contribute to breast cancer invasion. Cancer Res. *71*, 2455–2465.

Fleetwood, A.J., Cook, A.D., and Hamilton, J.A. (2005). Functions of granulocyte–macrophage colony-stimulating factor. Crit. Rev. Immunol. *25*, 405–428.

Gui, S.L., Teng, L.C., Wang, S.Q., et al. (2016). Overexpression of CXCL3 can enhance the oncogenic potential of prostate cancer. Int. Urol. Nephrol. *48*, 701–709.

Hamilton, J.A. (2020). GM-CSF in inflammation. J. Exp. Med. *217*, e20190945.

Hong, I.S. (2016). Stimulatory versus suppressive effects of GM-CSF on tumor progression in multiple cancer types. Exp. Mol. Med. *48*, e242.

Jung, K.H., Chu, K., Lee, S.T., et al. (2006). Granulocyte colony-stimulating factor stimulates neurogenesis via vascular endothelial growth factor with STAT activation. Brain Res. *1073–1074*, 190–201.

Kim, D.H., Sandoval, D., Reed, J.A., et al. (2008). The role of GM-CSF in adipose tissue inflammation. Am. J. Physiol. Endocrinol. Metab. *295*, E1038–E1046.

Kim, H.S., Jung, M., Choi, S.K., et al. (2018). IL-6-mediated cross-talk between human preadipocytes and ductal carcinoma in situ in breast cancer progression. J. Exp. Clin. Cancer Res. *37*, 200.

Lauby-Secretan, B., Scoccianti, C., Loomis, D., et al. (2016). Body fatness and cancer—viewpoint of the IARC Working Group. N. Engl. J. Med. *375*, 794–798.

Lee, B.Y., Timpson, P., Horvath, L.G., et al. (2015). FAK signaling in human cancer as a target for therapeutics. Pharmacol. Ther. *146*, 132–149.

Li, L., Li, Z., Lu, C., et al. (2022). Ibrutinib reverses IL-6-induced osimertinib resistance through inhibition of Laminin α5/FAK signaling. Commun. Biol. *5*, 155.

Liu, L., Wu, Y., Zhang, C., et al. (2020). Cancer-associated adipocyte-derived G-CSF promotes breast cancer malignancy via Stat3 signaling. J. Mol. Cell. Biol. *12*, 723–737.

Moreira, Â., Pereira, S.S., Costa, M., et al. (2015). Adipocyte secreted factors enhance aggressiveness of prostate carcinoma cells. PLoS One *10*, e0123217.

Pang, X., He, X., Qiu, Z., et al. (2023). Targeting integrin pathways: mechanisms and advances in therapy. Signal Transduct. Target. Ther. *8*, 1.

Pastushenko, I., and Blanpain, C. (2019). EMT transition states during tumor progression and metastasis. Trends Cell Biol. *29*, 212–226.

Picon-Ruiz, M., Morata-Tarifa, C., Valle-Goffin, J.J., et al. (2017). Obesity and adverse breast cancer risk and outcome: mechanistic insights and strategies for intervention. CA Cancer J. Clin. *67*, 378–397.

Qi, Y.L., Li, Y., Man, X.X., et al. (2020). CXCL3 overexpression promotes the tumorigenic potential of uterine cervical cancer cells via the MAPK/ERK pathway. J. Cell. Physiol. *235*, 4756–4765.

Reggiani, F., Labanca, V., Mancuso, P., et al. (2017). Adipose progenitor cell secretion of GM-CSF and MMP9 promotes a stromal and immunological microenvironment that supports breast cancer progression. Cancer Res. *77*, 5169–5182.

Revoltella, R.P., Menicagli, M., and Campani, D. (2012). Granulocyte-macrophage colony-stimulating factor as an autocrine survival–growth factor in human gliomas. Cytokine *57*, 347–359.

Reyes, N., Figueroa, S., Tiwari, R., et al. (2021). CXCL3 signaling in the tumor microenvironment. Adv. Exp. Med. Biol. *1302*, 15–24.

See, A.L., Chong, P.K., Lu, S.Y., et al. (2014). CXCL3 is a potential target for breast cancer metastasis. Curr. Cancer Drug Targets *14*, 294–309.

Sharma, P. (2016). Biology and management of patients with triple-negative breast cancer. Oncologist *21*, 1050–1062.

Su, X., Xu, Y., Fox, G.C., et al. (2021). Breast cancer-derived GM-CSF regulates arginase 1 in myeloid cells to promote an immunosuppressive microenvironment. J. Clin. Invest. *131*, e145296.

Tan, J., Buache, E., Chenard, M.P., et al. (2011). Adipocyte is a non-trivial, dynamic partner of breast cancer cells. Int. J. Dev. Biol. *55*, 851–859.

Thorn, M., Guha, P., Cunetta, M., et al. (2016). Tumor-associated GM-CSF overexpression induces immunoinhibitory molecules via STAT3 in myeloid-suppressor cells infiltrating liver metastases. Cancer Gene Ther. *23*, 188–198.

Wang, Z., Wang, Z., Li, G., et al. (2017). CXCL1 from tumor-associated lymphatic endothelial cells drives gastric cancer cell into lymphatic system via activating integrin β1/FAK/AKT signaling. Cancer Lett. *385*, 28–38.

Weng, J., Ren, Q., Li, Z., et al. (2021). CXCL3 overexpression affects the malignant behavior of oral squamous cell carcinoma cells via the MAPK signaling pathway. J. Oral Pathol. Med. *50*, 902–910.

Wilkinson, L., and Gathani, T. (2022). Understanding breast cancer as a global health concern. Br. J. Radiol. *95*, 20211033.

Wiseman, B.S., and Werb, Z. (2002). Stromal effects on mammary gland development and breast cancer. Science *296*, 1046–1049.

Wu, Q., Li, B., Li, Z., et al. (2019). Cancer-associated adipocytes: key players in breast cancer progression. J. Hematol. Oncol. *12*, 95.

Xiang, X., Ma, H.Z., Chen, Y.Q., et al. (2022). GM-CSF–miRNA–Jak2/Stat3 signaling mediates chemotherapy-induced cancer cell stemness in gastric cancer. Front. Pharmacol. *13*, 855351.

Xin, H., Cao, Y., Shao, M.L., et al. (2018). Chemokine CXCL3 mediates prostate cancer cells proliferation, migration and gene expression changes in an autocrine/paracrine fashion. Int. Urol. Nephrol. *50*, 861–868.

Zhang, L., Zhang, L., Li, H., et al. (2016). CXCL3 contributes to $CD133^+$ CSCs maintenance and forms a positive feedback regulation loop with CD133 in HCC via Erk1/2 phosphorylation. Sci. Rep. *6*, 27426.

Zhou, C., He, X., Tong, C., et al. (2022). Cancer-associated adipocytes promote the invasion and metastasis in breast cancer through LIF/CXCLs positive feedback loop. Int. J. Biol. Sci. *18*, 1363–1380.

Zhou, H., Zhang, Z., Qian, G., et al. (2020). Omentin-1 attenuates adipose tissue inflammation via restoration of TXNIP/NLRP3 signaling in high-fat diet-induced obese mice. Fundam. Clin. Pharmacol. *34*, 721–735.

Zhou, J., Yi, Q., and Tang, L. (2019). The roles of nuclear focal adhesion kinase (FAK) on cancer: a focused review. J. Exp. Clin. Cancer Res. *38*, 250.